JOC Article

Synthesis, Characterization, and Fluorescence Behavior of Twisted and Planar B_2N_2-Quaterphenyl Analogues

Cory A. Jaska,[†] Warren E. Piers,*[,†] Robert McDonald,[‡] and Masood Parvez[†]

Department of Chemistry, University of Calgary, 2500 University Drive N.W., Calgary, Alberta, Canada, T2N 1N4, and Department of Chemistry, University of Alberta, 11227 Saskatchewan Drive, Edmonton, Alberta, Canada T6G 2G2

wpiers@ucalgary.ca

Received March 30, 2007

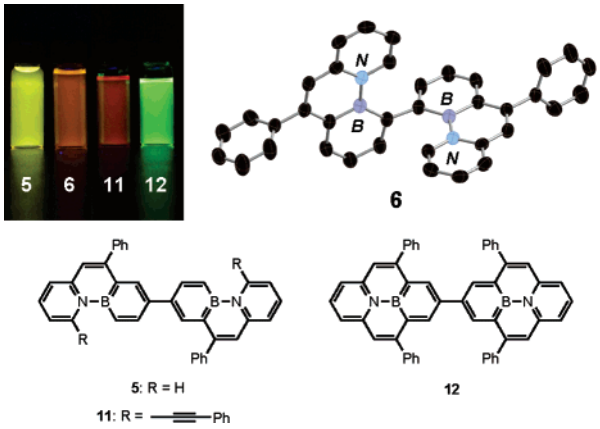

A series of planar and twisted heteroaromatic quaterphenyl analogues containing BN ring linkages has been synthesized using primarily difunctional Lewis acidic diborabiphenyl moieties as molecular cores. Crystal structure analyses indicated the presence of large twist angles between adjacent aromatic rings in **1** and **3**, which were also observed to possess nonfluorescent behavior due to a lack of molecular rigidity and insufficient B═N character in the excited state. In contrast, the incorporation of one or two bridging ethylene groups between the adjacent rings (installed via an ethynyl cycloisomerization) was found to afford planar phenanthrene or pyrene moieties, which resulted in weak fluorescence behavior (Φ_F = 0.02−0.16) for the *n*-Bu and Ph derivatives **5**−**12**. Emission colors ranged from green (λ_{em} = 521 nm) to red (λ_{em} = 630 nm) and depended primarily on the conformation (2,2′- vs 4,4′-), the extent of chromophore conjugation (phenanthrene vs pyrene), and the type of exocyclic substituent present (*n*-Bu vs Ph). Communication between the two phenanthrene or pyrene moieties was observed in some cases, which was characterized by bathochromically shifted emission bands relative to that of monomeric phenanthrene or pyrene species. Unique excited-state dimer (excimer) fluorescence was observed for the 2,2′-isomer **8**, which was characterized by broad, low-energy emission bands bathochromically shifted from that of the corresponding monomer.

Introduction

The phenylene oligomer *p*-quaterphenyl adopts a linear configuration through four para linked benzene rings and has been found to be a promising candidate in optoelectronic devices such as thin film transistors[1] and UV dye lasers[2] due to its blue light emission, chemical stability, high photoluminescence efficiency, and ability to form highly structured thin films via epitaxial growth methods.[3] While the higher oligomer *p*-

* Corresponding author. Tel.: (403) 220-5746; fax: (403) 289-9488.
[†] University of Calgary.
[‡] University of Alberta.

(1) Gundlach, D. J.; Lin, Y. -Y.; Jackson, T. N.; Schlom, D. G. *Appl. Phys. Lett.* **1997**, *71*, 3853.
(2) (a) Güsten, H.; Rinke, M.; Wirth, H. O. *Appl. Phys. B* **1988**, *45*, 279. (b) Nijegorodov, N. I.; Downey, W. S.; Danailov, M. B. *Spectrochim. Acta, Part A* **2000**, *56*, 783. (c) Hibino, R.; Nagawa, M.; Hotta, S.; Ichikawa, M.; Koyama, T.; Taniguchi, Y. *Adv. Mater.* **2002**, *14*, 119.

10.1021/jo0706574 CCC: $37.00
Published on Web 06/12/2007

sexiphenyl has found more common application in organic light-emitting diodes (LEDs)[4] due to a maximized effective conjugation length, examples of perfluorinated *p*-quaterphenyl analogues have also been shown to display efficient *n*-type semiconducting behavior.[5] In addition, oligomeric phenylenes have been utilized as model compounds in computational and experimental studies[6] on the effects of increasing chain length on the electronic and optical properties of poly(*p*-phenylene)s (PPPs),[7] a well-known class of conjugated polymers. While unsubstituted PPPs have been found to display high efficiencies and moderate charge carrier mobilities as the active layer in blue light-emitting polymer LEDs,[8] the use of ladder-type PPPs and the related poly(fluorene)s have become increasingly utilized as a result of the facile ability to tune the properties of the resulting materials. Variation of the bridging side-groups[7c,9] or polymer end-groups,[10] the incorporation of different bridging elements such as Si[11] or N,[12] or even the use of different counterions in polyelectrolytes[13] can all be utilized to modify the solubility, efficiency, and band gap to meet specific device criteria.[14] However, the most important function served by the bridging groups is that they induce the planarization of the molecular backbone, which can result in extended π-electron conjugation.

Our group has previously shown that by replacing aromatic C−C units with isoelectronic B−N moieties in pyrene,[15] phenanthrene,[16] and triphenylene-based systems,[17,18] significant bathochromic shifts were observed in the fluorescence spectra that resulted in emission in the visible region instead of the UV. Thus, it was anticipated that by substituting the ring C−C linkages of quaterphenyl by B−N bonds, similar effects on the fluorescence color and efficiency might occur. While this synthetic strategy has been previously utilized to provide BN analogues of biphenyl[19] and *p*-terphenyl,[20] no investigations on the photophysical properties (e.g., fluorescence) of the resulting materials have been performed to date. In this paper, we describe our efforts to synthesize a series of twisted and planar B_2N_2-analogues based on the quaterphenyl core and provide an in-depth investigation into their resulting structural and photophysical properties.

SCHEME 1

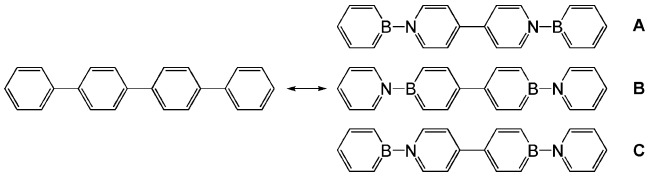

Results and Discussion

Synthesis of B_2N_2-Substituted *p*-Quaterphenyl and *o*-Quaterphenyl Analogues. As shown in Scheme 1, we identified **A** and **B** as two isomeric and isoelectronic B_2N_2-analogues of *p*-quaterphenyl for potential synthetic targets in this study. Isomer **A** possesses a 4,4′-bipyridine core capped by two borabenzene moieties, while isomer **B** possesses a 4,4′-diborabiphenyl core capped by two pyridine moieties. A third isomer **C** is also a plausible target, but while routes to **A** and **B** are readily envisioned, **C** would require the preparation of a 4,4′-borabenzenepyridine core that may be unstable with respect to self-condensation and the formation of undesirable oligomeric or polymeric species. Thus, we focused on the two isomers with opposing B−N dipoles in the present work.

Reaction of the commercially available 4,4′-bipyridine with 2 equiv of 1-chloro-4-isopropyl-2-trimethylsilylboracyclohexa-2,5-diene (**2,5-B**) was found to afford **1** (corresponding to **A**) as an air and moisture sensitive, dark blue solid in 84% yield. It was observed by multi-nuclear NMR that the formation of **1** proceeded slowly via an intermediate species **1′** (Scheme 2), which was formed immediately upon addition of the two reagents. Intermediate **1′** was identified as the *bis*-**2,5-B** adduct

(3) (a) Mikami, T.; Yanagi, H. *Appl. Phys. Lett.* **1998**, *73*, 563. (b) Yanagi, H.; Morikawa, T.; Fukushima, M.; Mikami, T. *Synth. Met.* **2001**, *121*, 1613.

(4) (a) Leising, G.; Tasch, S.; Brandstättter, C.; Meghdadi, F.; Froyer, G.; Athouel, L. *Adv. Mater.* **1997**, *9*, 33. (b) Niko, A.; Tasch, S.; Meghdadi, F.; Brandstättter, C.; Leising, G. *J. Appl. Phys.* **1997**, *82*, 4177. (c) Yanagi, H.; Okamoto, S. *Appl. Phys. Lett.* **1997**, *71*, 2563. (d) Meghdadi, F.; Tasch, S.; Winkler, B.; Fischer, W.; Stelzer, F.; Leising, G. *Synth. Met.* **1997**, *85*, 1441. (e) Yanagi, H.; Okamoto, S.; Mikami, T. *Synth. Met.* **1997**, *91*, 91. (f) Koch, N.; Pogantsch, A.; List, E. J. W.; Leising, G.; Blyth, R. I. R.; Ramsey, M. G.; Netzer, F. P. *Appl. Phys. Lett.* **1999**, *74*, 2909.

(5) (a) Winkler, B.; Meghdadi, F.; Tasch, S.; Müllner, R.; Resel, R.; Saf, R.; Leising, G.; Stelzer, F. *Opt. Mater.* **1998**, *9*, 159. (b) Sakamoto, Y.; Suzuki, T.; Miura, A.; Fujikawa, H.; Tokito, S.; Taga, Y. *J. Am. Chem. Soc.* **2000**, *122*, 1832. (c) Heidenhain, S. B.; Sakamoto, Y.; Suzuki, T.; Miura, A.; Fujikawa, H.; Mori, T.; Tokito, S.; Taga, Y. *J. Am. Chem. Soc.* **2000**, *122*, 10240.

(6) (a) Khanna, R. K.; Jiang, Y. M.; Creed, D. *J. Am. Chem. Soc.* **1991**, *113*, 5451. (b) Meerholz, K.; Heinze, J. *Electrochim. Acta* **1996**, *41*, 1839. (c) Heimel, G.; Pogantsch, A.; Zojer, E. *Phys. Scripta* **2004**, *109*, 156.

(7) For reviews on PPPs, see: (a) Tour, J. M. *Adv. Mater.* **1994**, *6*, 190. (b) Berresheim, A. J.; Müller, M.; Müllen, K. *Chem. Rev.* **1999**, *99*, 1747. (c) Grimsdale, A. C.; Müllen, K. *Adv. Polym. Sci.* **2006**, *199*, 1.

(8) (a) Grem, G.; Leditzky, G.; Ullrich, B.; Leising, G. *Adv. Mater.* **1992**, *4*, 36. (b) Grem, G.; Leditzky, G.; Ullrich, B.; Leising, G. *Synth. Met.* **1992**, *51*, 383.

(9) (a) Li, J. Y.; Ziegler, A.; Wegner, G. *Chem.—Eur. J.* **2005**, *11*, 4450. (b) Mallavia, R.; Montilla, F.; Pastor, I.; Velásquez, P.; Arredondo, B.; Álvarez, A. L.; Mateo, C. R. *Macromolecules* **2005**, *38*, 3185.

(10) (a) Miteva, T.; Meisel, A.; Knoll, W.; Nothofer, H. G.; Scherf, U.; Müller, D. C.; Meerholz, K.; Yasuda, A.; Neher, D. *Adv. Mater.* **2001**, *13*, 565. (b) Hung, M. C.; Liao, J. L.; Chen, S. A.; Chen, S. H.; Su, A. C. *J. Am. Chem. Soc.* **2005**, *127*, 14576. (c) Li, Z. H.; Wong, M. S.; Tao, Y.; Lu, J. *Chem.—Eur. J.* **2005**, *11*, 3285.

(11) (a) Chan, K. L.; McKiernan, M. J.; Towns, C. R.; Holmes, A. B. *J. Am. Chem. Soc.* **2005**, *127*, 7662. (b) Mo, Y.; Tian, R.; Shi, W.; Cao, Y. *Chem. Commun.* **2005**, 4925. (c) Chan, K. L.; Watkins, S. E.; Mak, C. S. K.; McKiernan, M. J.; Towns, C. R.; Pascu, S. I.; Holmes, A. B. *Chem. Commun.* **2005**, 5766. (d) Usta, H.; Lu, G.; Facchetti, A.; Marks, T. J. *J. Am. Chem. Soc.* **2006**, *128*, 9034. (e) Zhang, X.; Jiang, C.; Mo, Y.; Xu, Y.; Shi, H.; Cao, Y. *Appl. Phys. Lett.* **2006**, *88*, 51116.

(12) (a) Morin, J.-F.; Leclerc, M. *Macromolecules* **2001**, *34*, 4680. (b) Morin, J. F.; Leclerc, M. *Macromolecules* **2002**, *35*, 8413. (c) Jung, S. H.; Pisula, W.; Rouhanipour, A.; Räder, H. J.; Jacob, J.; Müllen, K. *Angew. Chem., Int. Ed.* **2006**, *45*, 4685. (d) Li, Y.; Wu, Y.; Ong, B. S. *Macromolecules* **2006**, *39*, 6521. (e) Iraqi, A.; Pickup, D. F.; Yi, H. *Chem. Mater.* **2006**, *18*, 1007.

(13) Yang, R.; Wu, H.; Cao, Y.; Bazan, G. C. *J. Am. Chem. Soc.* **2006**, *128*, 14422.

(14) Short-chain molecular fluorenes have also been used in OLED devices; see: (a) Chao, T. C.; Lin, Y. T.; Yang, C. Y.; Hung, T. S.; Chou, H. C.; Wu, C. C.; Wong, K. T. *Adv. Mater.* **2005**, *17*, 992. (b) Hadizad, T.; Zhang, J.; Wang, Z. Y.; Gorjanc, T. C.; Py, C. *Org. Lett.* **2005**, *7*, 795. (c) Wong, K. T.; Chen, R. T.; Fang, F. C.; Wu, C. C.; Lin, Y. T. *Org. Lett.* **2005**, *7*, 1979. (d) Li, Z. H.; Wong, M. S.; Fukutani, H.; Tao, Y. *Org. Lett.* **2006**, *8*, 4271. (e) Locklin, J.; Ling, M. M.; Sung, A.; Roberts, M. E.; Bao, Z. *Adv. Mater.* **2006**, *18*, 2989.

(15) Bosdet, M. J. D.; Sorensen, T. S.; Piers, W. E.; Parvez, M. *Angew. Chem., Int. Ed.* **2007**, DOI: 10.1002/anie.200700591.

(16) Bosdet, M. J. D.; Jaska, C. A.; Piers, W. E.; Sorensen, T. S.; Parvez, M. *Org. Lett.* **2007**, *9*, 1395.

(17) Emslie, D. J. H.; Piers, W. E.; Parvez, M. *Angew. Chem., Int. Ed.* **2003**, *42*, 1252.

(18) Jaska, C. A.; Emslie, D. J. H.; Bosdet, M. J. D.; Piers, W. E.; Sorensen, T. S.; Parvez, M. *J. Am. Chem. Soc.* **2006**, *128*, 10885.

(19) Boese, R.; Finke, N.; Henkelmann, J.; Maier, G.; Paetzold, P.; Reisenauer, H. P.; Schmid, G. *Chem. Ber.* **1985**, *118*, 1644.

(20) Qiao, S.; Hoic, D. A.; Fu, G. C. *Organometallics* **1997**, *16*, 1501.

SCHEME 2

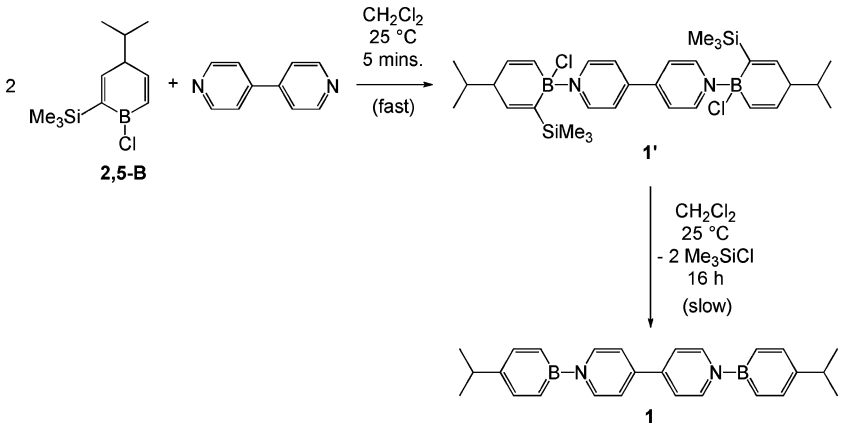

SCHEME 3

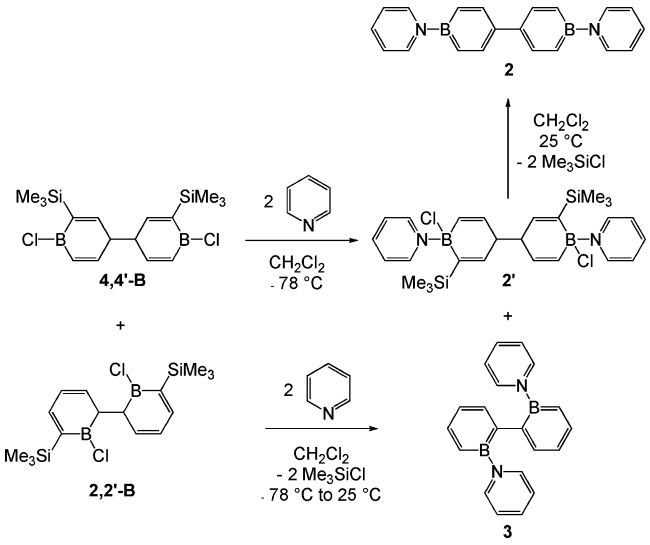

SCHEME 4

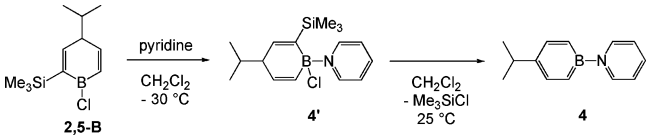

of 4,4′-bipyridine, as evidenced by a new resonance in the ^{11}B NMR spectrum at 3.1 ppm, which is in a region characteristic of four-coordinate boron.[21] In addition, slightly shifted ^{1}H NMR resonances for the boracycle ring protons were observed, in particular, the presence of a multiplet at 2.82 ppm due to the hydrogen atom on the sp^3 carbon located para to the boron. Intermediate **1′** was observable due to a prerequisite but slow 1,3-hydrogen shift in the 2,5-diene regioisomer to give the 3,5-diene, which can then rapidly eliminate Me_3SiCl and aromatize to afford the borabenzene.[22] Complete conversion of **1′** to **1** typically took ca. 8 h at 25 °C and was accompanied by a new resonance in the ^{11}B NMR spectrum at 31.2 ppm, which is in a region typical of borabenzene·pyridine adducts (cf. 33.9 ppm in **BB-py**).[19]

The inverse isomer of **1** (corresponding to **B**), where the boron and nitrogen atoms are mutually exchanged, was subsequently prepared by the reaction of 4,4′-bi(boracyclohexa-2,5-diene) **4,4′-B** (as a 40:60 mixture with the isomeric 2,2′-bi(boracyclohexa-3,5-diene) **2,2′-B**)[18] with 2 equiv of pyridine, which afforded both the desired *p*-quaterphenyl analogue **2** and also the *o*-quaterphenyl analogue **3** (Scheme 3) as evidenced by a broad ^{11}B NMR resonance at 31.3 ppm. As in the case of **1**, an intermediate species **2′** was observed that corresponded to the bis-pyridine adduct of **4,4′-B**. While the conversion of **2′** to **2** required ca. 8 h for completion, the reaction of **2,2′-B** with pyridine proceeded instantaneously to afford species **3** without any observable intermediate. This reactivity is due the facile nature of the 1,5-hydrogen shift in the 3,5-diene regioisomer of **2,2′-B** as compared to the 1,3-hydrogen shift in the 2,5-diene **4,4′-B**.[23] Quaterphenyls **2** and **3** were isolated as air and moisture sensitive, purple−black, and dark red solids, respectively, after successive recrystallizations. In addition, it was observed that solutions of **1**−**3** were prone to decomposition in the presence of protic impurities, which hindered their overall stability in solution over extended time periods. It is likely that the instability of **1**−**3** is due in part to the sterically uncongested B−N bond, where small molecule impurities can readily add across the highly reactive B═C double bond or break the dative B ← N bond, leading to rapid decomposition of uncoordinated borabenzene species.

To confirm the structures of proposed intermediates **1′** and **2′**, a pyridine adduct of a singly borocyclic model compound was prepared. Reaction of **2,5-B** with 1 equiv of pyridine in CD_2Cl_2 at 25 °C was found to immediately afford the initial four-coordinate boron adduct species **4′** (Scheme 4), similar to the observed reactivity of **4,4′-B**. The ^{1}H NMR spectrum of **4′** showed a resonance due to the proton on the sp^3 carbon atom located para to the boron and three more olefinic resonances downfield in a similar arrangement to that of unreacted **2,5-B**. The ^{11}B NMR spectrum of **4′** showed a broad resonance at 2.9 ppm in a region characteristic of four-coordinate boron.[21] The ESI-MS of **4′** showed a signal at $m/z = 228$ corresponding to $M^+ - Cl$, which indicated the presence of a B ← N dative bond

(21) Nöth, H.; Wrackmeyer, B. *NMR: Basic Princ. Prog.* **1978**, *14*, 1.
(22) Hoic, D. A.; Wolf, J. R.; Davis, W. M.; Fu, G. C. *Organometallics* **1996**, *15*, 1315.

(23) In contrast to 1,3-hydrogen shifts, 1,5-hydrogen shifts in simple cyclic systems are slow due to relatively high activation energies: (a) Hess, B. A., Jr.; Baldwin, J. E. *J. Org. Chem.* **2002**, *67*, 6025. However, 1,5-hydrogen shifts have been observed experimentally to proceed rapidly with low barriers when the product contains multiple aromatic rings: (b) Lewis, F. D.; Zuo, X.; Gevorgyan, V.; Rubin, M. *J. Am. Chem. Soc.* **2002**, *124*, 13664. The reduction or disappearance of these activation barriers has also be verified computationally: (c) Alabugin, I. V.; Manoharan, M.; Breiner, B.; Lewis, F. D. *J. Am. Chem. Soc.* **2003**, *125*, 9329.

SCHEME 5

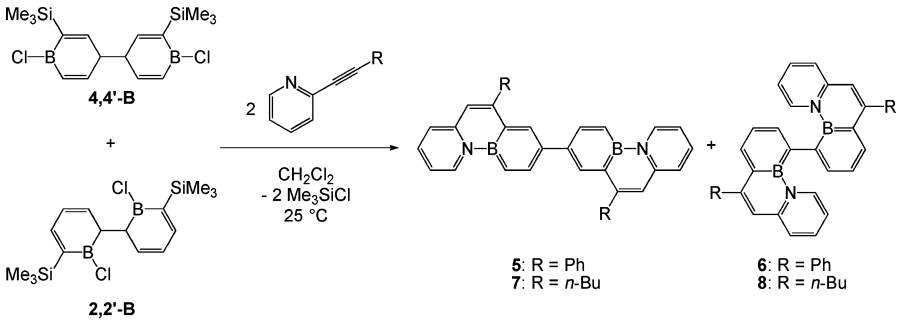

and confirmed the connectivity. The intermediate **4′** was observed to react further at 25 °C, undergoing a 1,3-hydrogen shift with concomitant Me_3SiCl elimination over ca. 8 h in solution to form the known borabenzene-pyridine adduct **4**.[24] The nature of **4′** was further established via a crystal structure determination, details of which are presented in the Supporting Information.

Since **1**−**3** were found to be unstable over prolonged time periods, the incorporation of a bridging group that could provide additional steric protection to the reactive boron center, while also helping to enforce planarity between the adjacent rings, was determined to be a desirable synthetic goal. This has been a common strategy in the synthesis of ladder-type PPPs and poly(fluorene)s, where bridging groups can be utilized to adjust the emission properties and solubility of the resulting materials.[7c] Fortunately, our group has found that ethylene bridges can be easily installed at the α position of the borabenzene ring via the cycloisomerization reaction of an alkyne moiety located at the ortho position of the pyridine ring.[15,16] For mono- and di-substituted pyridines, it was found that the first cycloisomerization reaction proceeded spontaneously at 25 °C,[15,16,25,26] while the second isomerization reaction in 2,6-di-substituted pyridines typically required a catalyst (e.g., $PtCl_2$) and heat (80 °C) to ensure complete closure and encapsulation of the B−N fragment.[15] Thus, the reaction of **4,4′-B**/**2,2′-B** with either 2-(hex-1-ynyl)pyridine or 2-(phenylethynyl)pyridine was found to afford the linked species **5**−**8** (Scheme 5), which can be regarded as B_2N_2-analogues of either 2,2′-biphenanthrenyl (**5** and **7**) or 4,4′-biphenanthrenyl (**6** and **8**). The reaction likely proceeds initially via coordination of the pyridine moiety (similar in structure to **2′**), followed by a 1,3-hydrogen shift and elimination of Me_3SiCl to afford the borabezene species, which finally undergoes cycloisomerization with the ethynyl group to provide **5**−**8**. Fortunately, the ethylene bridges were found to enhance both the solubility and the stability of the quaterphenyl cores in **5**−**8**, which allowed the use of column chromatography for separation and purification of the 4,4′- and 2,2′-isomers. The 4,4′-isomers **5** and **7** and the 2,2′-isomers **6** and **8** were all isolated in good yields (64−76%) as either red or orange solids and possessed ^{11}B NMR resonances in the range of 27.6−29.1 ppm.

SCHEME 6

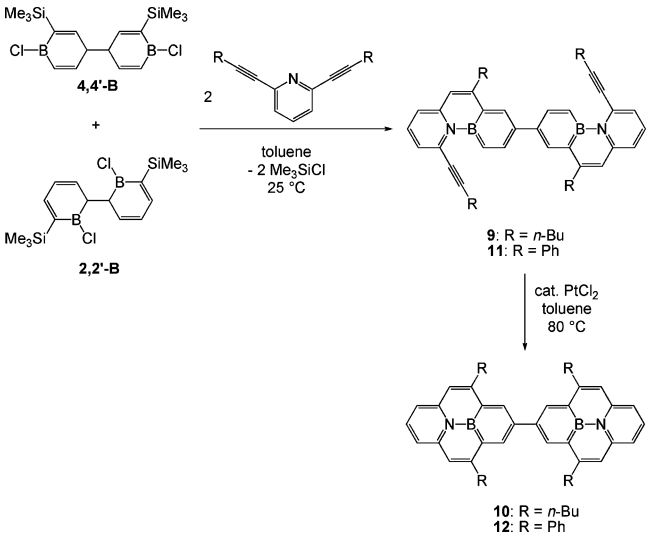

To further enhance the stability, as well as to increase the potential conjugation of the molecule, the reaction of **4,4′-B**/**2,2′-B** with either 2,6-bis-(hex-1-ynyl)-pyridine or 2,6-bis-(phenylethynyl)-pyridine was performed to achieve a B_2N_2-substituted bipyrene analogue. The reaction was found initially to afford only the half-isomerized 4,4′-species **9** and **11**, which were isolated as red−purple solids after column chromatography (Scheme 6). Unfortunately, the fate of the 2,2′-component **2,2′-B** was not determined in these reactions. The **2,2′-B** species could potentially form a half-isomerized species analogous to **9** and **11**, but the second cycloisomerization would be prevented from occurring due to blockage of the other α position of the borabenzene ring as a result of the 2,2′-junction point. However, formation of a phenanthrene-type ring analogous to **6** and **8** should result in a species that is stable to column chromatography, which was not observed in this case. Instead, it is likely that cycloisomerization did not occur in the 2,2′-component due to an unfavorable geometry, as steric repulsion between the alkyne moiety and the second borabenzene ring would effectively prevent the required coplanar arrangement of the pyridine and borabenzene rings prior to isomerization. Thus, decomposition of the most likely product, namely, the unlinked borabenzene·pyridine adduct, was observed to afford the free pyridine upon attempted purification of the crude reaction mixture via chromatography.

(24) Ghesner, I.; Piers, W. E.; Parvez, M.; McDonald, R. *Chem. Commun.* **2005**, 2480.

(25) The cycloisomerization of the pendant ethynyl group was found to be unusually facile, as similar transformations in all-carbon or other heteroaromatic systems are typically incurred via a soft metal catalyst, UV irradiation, or flash vacuum pyrolysis. The observed increase in reactivity in this case may be due to the enhanced nucleophilic nature of the carbon atom α to boron. See ref 24 and Pan, J.; Kampf, J. W.; Ashe, A. J., III. *Org. Lett.* **2007**, *9*, 679.

(26) This general mode of reactivity has been observed with a variety of substituents on the alkyne (e.g., H, *n*-Bu, or Ph). However, this reaction is not spontaneous when the alkyne is substituted with $SiMe_3$, resulting in predominant formation of the 1:1 borabenzene·pyridine adduct at 25 °C. From this adduct, the subsequent cycloisomerization has been observed to proceed very slowly at 25 °C in the absence of a catalyst or very rapidly in the presence of a catalyst.

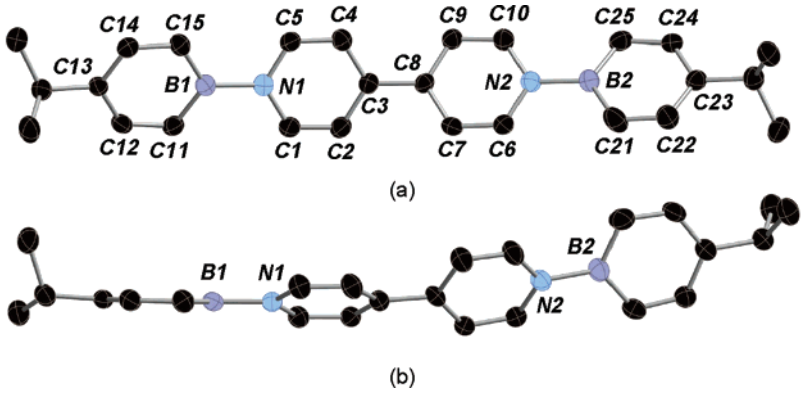

FIGURE 1. (a) Molecular structure of **1**. All hydrogen atoms have been omitted for clarity. Selected bond lengths (angstroms): B(1)−N(1) 1.546(4), B(2)−N(2) 1.551(4), B(1)−C(11) 1.494(5), C(11)−C(12) 1.386(4), C(12)−C(13) 1.392(4), C(13)−C(14) 1.390(4), C(14)−C(15) 1.393-(4), B(1)−C(15) 1.475(5), N(1)−C(1) 1.355(4), C(1)−C(2) 1.364(4), C(2)−C(3) 1.393(5), C(3)−C(4) 1.390(4), C(4)−C(5) 1.369(4), N(1)−C(5) 1.353(4), and C(3)−C(8) 1.476(4) and twist angles (deg): $C_5B(1)-C_5N(1)$ 19.7, $C_5N(1)-C_5N(2)$ 28.6, and $C_5N(2)-C_5B(2)$ 21.7. (b) View of **1** that displays the helical twist along the backbone.

Heating species **9** or **11** at 80 °C in the presence of a catalytic amount of $PtCl_2$ was found to afford the fully isomerized species **10** or **12**, which were isolated as orange solids in moderate yields (57−67%) after column chromatography (Scheme 6). The ^{11}B NMR spectra of **10** and **12** displayed broad singlets centered at 21.8 and 23.3 ppm, respectively, slightly shifted upfield from that of their isomeric precursors **9** and **11** (29.3 and 28.5 ppm). Unfortunately, X-ray quality crystals of **9**−**12** could not be obtained even after several repeated attempts, due to the preferred formation of thin needles comprised of microcrystalline layers.

Structural Analysis of B_2N_2-Substituted *p*-Quaterphenyl and *o*-Quaterphenyl Analogues. The molecular structure of **1** was confirmed by X-ray crystallography and is shown in Figure 1a. The four aromatic borabenzene and pyridine rings in **1** were found to be planar with delocalized C═C double bonds, along with the presence of large twist angles (19.7, 28.6, and 21.7°) between adjacent rings that resulted in a partial helical twist along the molecule's long axis (Figure 1b). This type of helical twist is in contrast to the two reported crystal polymorphs of *p*-quaterphenyl in which the rings were found to be alternately twisted along the backbone.[27] The B−N dative bond lengths were found to be 1.546(4) and 1.551(4) Å, with a C(3)−C(8) bond length of 1.476(4) Å between the central pyridine rings (cf. 1.484 Å in 4,4′-bipyridine).[28] In comparison, the B−N bond lengths in the BN analogues of biphenyl[19] and *p*-terphenyl[20] were determined to be 1.56 and 1.55 Å, respectively. These species were also observed to possess much larger twist angles between adjacent rings than were found in **1**, with values of 43° for the biphenyl analogue and 49° (C_5B-NC_5) and 43° (NC_5-C_6) for the *p*-terphenyl analogue, which also possessed alternately twisted rings. While herringbone packing motifs have been observed in *p*-quaterphenyl through close edge carbon-to-π-face interactions,[27] both the helical twist and the bulky *i*Pr groups combine to prevent this type of extended solid-state assembly in **1**.

The molecular structure of **3** (Figure 2) was observed to possess four planar, aromatic rings with delocalized C═C bonds and very large twist angles (48.3, 125.8, and 56.5°) between the adjacent rings. As in the case of **1**, B−N bond lengths of

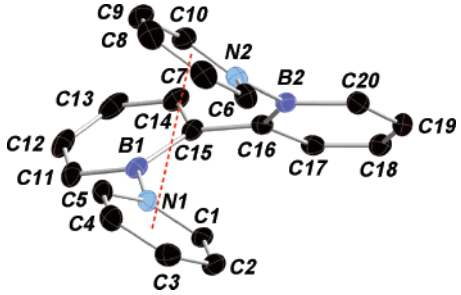

FIGURE 2. Molecular structure of **3**. All hydrogen atoms have been omitted for clarity. Selected bond lengths (angstroms): B(1)−N(1) 1.550(3), B(2)−N(2) 1.554(3), B(1)−C(11) 1.485(4), C(11)−C(12) 1.389(4), C(12)−C(13) 1.388(4), C(13)−C(14) 1.405(4), C(14)−C(15) 1.407(3), B(1)−C(15) 1.504(4), N(1)−C(1) 1.352(3), C(1)−C(2) 1.368-(3), C(2)−C(3) 1.387(3), C(3)−C(4) 1.382(4), C(4)−C(5) 1.373(4), N(1)−C(5) 1.356(3), C(15)−C(16) 1.494(3), and (pyridine)···(pyridine) 3.58 and twist angles (deg): $C_5N(1)-C_5B(1)$ 48.3, $C_5B(1)-C_5B(2)$ 125.8, and $C_5B(2)-C_5N(2)$ 56.5.

1.550(3) and 1.554(3) Å were found (cf. 1.546(4) and 1.551(4) Å in **1**), while the C(15)−C(16) bond length was found to be 1.494(3) Å (cf. 1.476(4) Å in **1**). The most notable feature in **3** was the presence of an intramolecular π-stacking interaction between the two pyridine rings (closest contact ca. 3.58 Å) that arises as a result of a cis geometrical arrangement of the two Lewis acidic boron centers.

The molecular structure of **6** (Figure 3a) was found to consist of two planar BN-phenanthrene moieties situated nearly perpendicular to each other (88.4°) and to the exocyclic phenyl groups (84.9°). The B−N bond length was found to be 1.493-(2) Å, significantly shorter than those found in either **1** (1.546-(4) and 1.551(4) Å) or **3** (1.550(3) and 1.554(3) Å) but longer than those found in the heteroaromatic B_2N_2-triphenylene (1.464(4) Å)[18] or BN-pyrene (1.456(4) Å)[15] analogues. This bond length is the same as that found in the structure of BN-Ph-phenanthrene (1.489(2) Å)[16] and suggests that some degree of B═N double bond character exists in **6**. The C(1)−C(1*) bond length of 1.510(3) Å was found to be slightly longer than that of **1** (1.476(4) Å) or **3** (1.494(3) Å), likely due to the

(27) (a) Baudour, J. L.; Delugeard, Y.; Cailleau, H. *Acta Crystallogr., Sect. B:Struct. Sci.* **1976**, *32*, 150. (b) Baudour, J. L.; Delugeard, Y.; Rivet, P. *Acta Crystallogr., Sect. B: Struct. Sci.* **1978**, *34*, 625.

(28) Boag, N. M.; Coward, K. M.; Jones, A. C.; Pemble, M. E.; Thompson, J. R. *Acta Crystallogr., Sect. C:Cryst. Struct. Commun.* **1999**, *55*, 672.

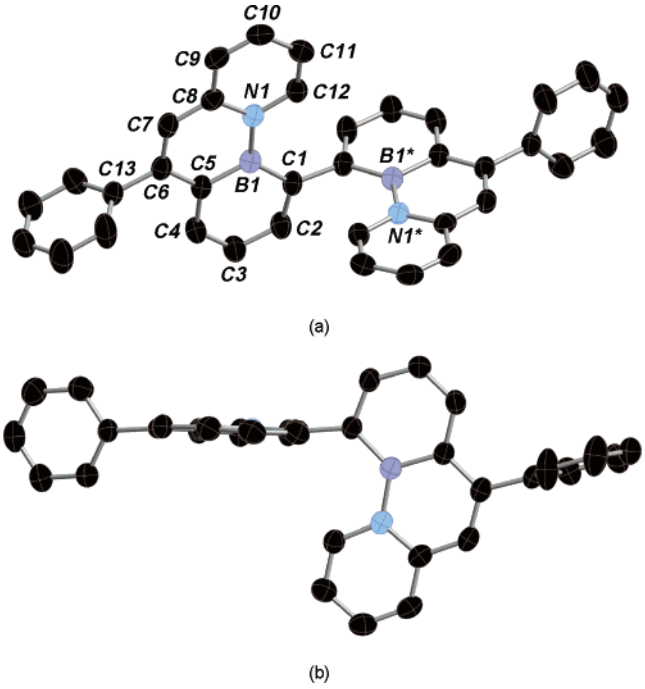

FIGURE 3. (a) Molecular structure of **6**. All hydrogen atoms have been omitted for clarity. Selected bond lengths (angstroms): B(1)−N(1) 1.493(2), B(1)−C(1) 1.531(2), C(1)−C(2) 1.376(2), C(2)−C(3) 1.420(2), C(3)−C(4) 1.363(2), C(4)−C(5) 1.425(2), B(1)−C(5) 1.516-(3), C(5)−C(6) 1.418(2), C(6)−C(7) 1.376(2), C(7)−C(8) 1.402(2), N(1)−C(8) 1.390(2), C(8)−C(9) 1.418(2), C(9)−C(10) 1.355(3), C(10)−C(11) 1.408(3), C(11)−C(12) 1.351(2), N(1)−C(12) 1.386(2), C(1)−C(1*) 1.510(3); twist angles (deg): $C_5N(1)-C_5B(1)$ 4.3, C_5B-$(1)-C_5B(1^*)$ 88.4, Ph−C_4BN 84.9; and torsion angles (deg): C(1)−B(1)−N(1)−C(12) −2.9(2), C(1)−B(1)−N(1)−C(8) −179.5(1), C(5)−B(1)−N(1)−C(8) −0.4(2), C(5)−B(1)−N(1)−C(12) 176.2(1), and C(5)−C(6)−C(7)−C(8) −2.0(3). (b) View of **6** that displays the perpendicular arrangement of the planar rings.

increased steric repulsion between the two bulky phenanthrene moieties. In the carbon framework periphery of the phenanthrene moiety, the C═C double bonds were found to be partially localized with alternating longer (average 1.42 Å) and shorter bond lengths (average 1.36 Å), a similar type of bonding arrangement to that found in both BN-Ph-phenanthrene[16] and B_2N_2-triphenylene.[18] Because of the perpendicular arrangement of the planar rings (Figure 3b), no significant π-stacking interactions were observed in the extended solid-state structure.

Photophysical Properties of B_2N_2-Substituted *p*-Quaterphenyl and *o*-Quaterphenyl Analogues. (a) Photophysical Properties of 1−3. It has been previously observed that the all-carbon phenylene series displays fluorescent behavior with moderate to high quantum yields: biphenyl (λ_{em} = 305 nm, Φ_F = 0.17−0.25), *p*-terphenyl (λ_{em} = 338 nm, Φ_F = 0.84−0.88), *o*-quaterphenyl (λ_{em} = 396 nm), and *p*-quaterphenyl (λ_{em} = 407 nm, Φ_F = 0.81).[2b,29] The biphenyl derivatives with one and two ethylene bridges are also fluorescent, with red-shifted emission maxima and higher quantum yields than biphenyl as a result of a larger and more rigid aromatic system: phenanthrene (λ_{em} = 346 nm, Φ_F = 0.31) and pyrene (λ_{em} = 372 nm, Φ_F = 0.60).[29b] While examples of 2,2′-biphenanthrenyl, 4,4′-biphenanthrenyl, and 2,2′-bipyrene have all been previously synthesized (albeit, usually as a component in a complex mixture of products), no photophysical data for these species have been reported in the literature to date.[30] However, the biphenyl analogue **BB-py**, the *p*-terphenyl analogue **BB-py-Ph**, the isomeric *p*-quaterphenyl analogues **1** and **2**, as well as the bent *o*-quaterphenyl analogue **3** were all observed to display no fluorescence behavior. This may be due in part to a lack of rigidity in the molecule, which would support radiationless deactivation pathways and thus inhibit fluorescence behavior. In addition, biphenyl, *p*-terphenyl, and *p*-quaterphenyl are also expected to possess more pronounced double bond character in the $C(sp^2)-C(sp^2)$ bonds between aromatic rings in the excited state,[29b] which would help contribute to the molecular rigidity and thus fluorescence behavior. As fluorescent behavior was not observed in the BN-analogues, it is likely that the B−N bonds do not possess any significant double bond character in either the ground or the excited state.

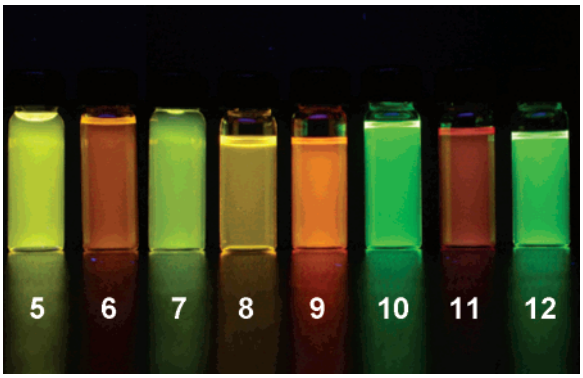

FIGURE 4. Fluorescence of cyclohexane solutions of **5**−**12** upon irradiation at 365 nm.

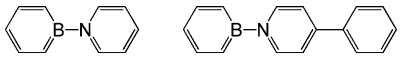

BB-py **BB-py-Ph**

As discussed previously, however, the X-ray structural analysis of ethylene-bridged species such as phenanthrene (e.g., **6**) and pyrene[15] clearly indicates the presence of some B═N double bond character in the ground state, which should result in more planar species in the excited state and may result in fluorescent behavior. Indeed, irradiation of species **5**−**12** at 365 nm was found to result in fluorescence in the visible region (Figure 4 and Table 1).

(b) Fluorescence Emission of 5 and 6. Beginning with the case of the Ph-substituted derivatives, the linear 4,4′-species **5** was observed to possess an emission maximum at 568 nm, whereas the bent 2,2′-species **6** was found to be red-shifted by 23 nm with an emission maximum at 591 nm (Figure 5). This is in contrast to the behavior exhibited by the linear *p*-quaterphenyl and the bent *o*-quaterphenyl, in which the latter is blue-shifted by 11 nm due to slightly reduced conjugation.

(29) (a) Jurgensen, A.; Inman, E. L., Jr.; Winefordner, J. D. *Anal. Chim. Acta* **1981**, *131*, 187. (b) Nijegorodov, N. I.; Downey, W. S. *J. Phys. Chem.* **1994**, *98*, 5639. (c) Uchida, K.; Kakei, T.; Takahashi, Y. *J. Lumin.* **1997**, *72*−*74*, 501.

(30) For 2,2′-biphenanthrenyl: (a) Lang, K. F.; Buffleb, H.; Kalowy, J. *Chem. Ber.* **1960**, *93*, 303. (b) Badger, G. M.; Donnelly, J. K.; Spotswood, T. M. *Aust. J. Chem.* **1960**, *17*, 1138. (c) Shih, H. T.; Shih, H. H.; Cheng, C. H. *Org. Lett.* **2001**, *3*, 811. For 4,4′-biphenanthrenyl: (d) Dore, A.; Fabbri, D.; Gladiali, S.; Valle, G. *Tetrahedron: Asymmetry* **1995**, *6*, 779. For 2,2′-bipyrene: (e) Mukherjee, J.; Sarofim, A. F.; Longwell, J. P. *Combust. Flame* **1994**, *96*, 191. An example of a 2,2′,2″-terphenanthrenyl has recently been reported: Tian, H.; Shi, J.; Dong, S.; Yan, D.; Wang, L.; Geng, Y.; Wang, F. *Chem. Commun.* **2006**, 3498.

TABLE 1. UV−vis, Fluorescence, Quantum Yield, and Lifetime Data for 5−12[a]

	UV−vis[b] (nm)	fluorescence[c] (nm) [color]	$\Delta\nu$[d] (cm^{-1}) [nm]	Φ_F[e]	τ_F[f] (ns)
5	517	568 [yellow]	1737 [51]	0.16	4.0
6	449, 424	591 [orange−red]	5352 [142]	0.02	4.5
7	512, 490	543, 558 [yellow−green]	1115 [31]	0.05	3.5
8	446	451, 475 (monomer) 566 (excimer) [yellow−orange]	249 [5]	0.03 0.05	4.3 23.3
9	523	598 [orange−red]	2398 [75]	0.12	4.0
10	426	550 [green]	5292 [124]	0.06	20.5
11	546, 401	630 [red]	2442 [84]	0.02	2.4
12	444	521 [green]	3329 [77]	0.12	25.8

[a] All experiments were performed in cyclohexane. [b] Only the bands in the visible region are reported. See the Experimental Section for more details. [c] Excitation at either 260 or 330 nm. [d] $\Delta\nu$ = Stokes shift. [e] Φ_F = Quantum yield. Quantum yields are reported relative to 9,10-diphenylanthracene ($\Phi_F = 0.90$). [f] τ_F = Fluorescence lifetime.

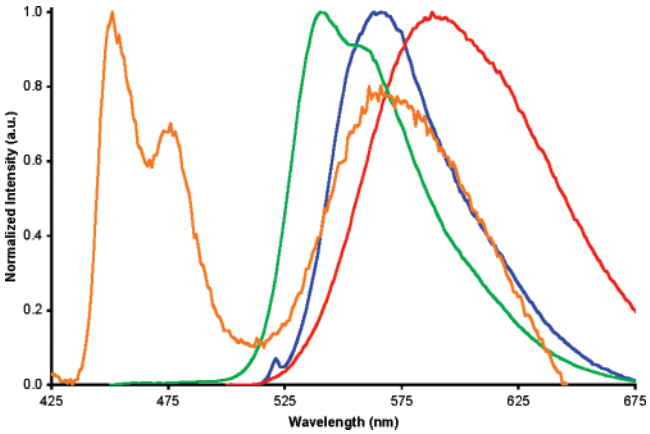

FIGURE 5. Fluorescence emission spectra of **5** (blue), **6** (red), **7** (green), and **8** (orange).

The Stokes shifts for **5** and **6** were observed to be 51 and 142 nm, respectively, which are comparable to those observed for their closest structural analogues *p*-quaterphenyl (ca. 75 nm) and *o*-quaterphenyl (148 nm). These values imply that in the excited state, there is a more pronounced geometric distortion in the structure of **6** as compared to that of **5**. This distortion may be attributed to an increase in steric hindrance about an ortho linkage relative to that of a para linkage, as the two middle rings in **6** are nearly perpendicular to one another. Thus, these two rings would be required to undergo a significant twist to achieve a more coplanar conformation, which would allow for more C═C double bond character (of the critical ring-linking BC_5-C_5B bond) in the excited state. In contrast, a more coplanar conformation for **5** would be expected due to less severe steric interactions and thus would not have to distort to a great extent to allow for increased C═C character in the excited state, resulting in a lower Stokes shift value. In addition, the quantum yield of the linear **5** was determined to be 0.16 with a lifetime of 4.0 ns, while the quantum yield of the bent **6** was much lower at 0.02 with a comparable lifetime of 4.5 ns. In comparison to the uncoupled BN-Ph-phenanthrene species ($\lambda_{em} = 459$ nm, $\Phi_F = 0.49$),[16] the emission bands in **5** and **6** are dramatically red-shifted by 109 and 132 nm, respectively, which is suggestive of some degree of communication between the phenanthrene moieties that results in a longer effective conjugation length. However, this extended conjugation comes at the expense of increased nonradiative pathways, as the quantum yields are substantially reduced in value.

The effect of solvent polarity on the fluorescence emission of **5** and **6** were also investigated. However, the emission bands in **5** were found to be essentially invariant when recorded in cyclohexane ($\epsilon = 2.0$), toluene ($\epsilon = 2.4$), Et_2O ($\epsilon = 4.3$), THF ($\epsilon = 7.5$), CH_2Cl_2 ($\epsilon = 9.1$), or CH_3CN ($\epsilon = 37.5$) (Figure S10, Supporting Information). This implies that the fluorophore has little or no change in the dipole moment between the ground and the excited states, as nonpolar molecules usually display little sensitivity toward solvent polarity. Similar solvent behavior was also observed for **6** (Figure S11, Supporting Information).

(c) Fluorescence Emission of 7 and 8. In the case of the linear 4,4′-*n*-Bu derivative **7**, an emission maximum at 543 nm was observed, which was found to be blue-shifted by 25 nm as compared to that of the analogous Ph derivative **5** (Figure 5). This is due to exocyclic conjugation effects, as replacement of the aromatic phenyl groups with *n*-butyl substituents will reduce the overall conjugation of the chromophore leading to an expected blue-shift in the emission band. In addition, the Stokes shift, quantum yield, and lifetime for **7** were found to be 31 nm and 0.05 and 3.5 ns, respectively. These values are comparable to those found for **5** with the exception of the quantum yield, which was determined to be lower in **7** (0.05 vs 0.16). In comparison to the uncoupled BN-*n*-Bu-phenanthrene ($\lambda_{em} = 456$ nm, $\Phi_F = 0.56$),[16] the emission maximum in **7** was found to be red-shifted by 87 nm, which is again suggestive of communication between the phenanthrene moieties, while the quantum yield was again determined to be substantially lower.

In contrast to **6**, the bent 2,2′-*n*-Bu derivative **8** displayed different emission behavior with the presence of two emission bands at 451 and 566 nm (Figure 5). The band at 451 nm was observed to have a similar mirror image fine structure as that seen in the absorption spectrum with a rather small Stokes shift value of 5 nm. The low-energy band (566 nm) was found to be broad and featureless as well as concentration-dependent, as the intensity was observed to decrease at the expense of the high-energy band (451 nm) upon increased dilution. For example, at high concentrations (10^{-5} M), only the 566 nm band was present, while at low concentrations (10^{-8} M), the band at 451 nm was the dominant feature (Figure 6). This type of concentration-dependence is suggestive of excimer fluorescence,[31] with emission occurring from an excited-state dimeric complex resulting in the low-energy band at 566 nm. The formation of an excimer (e.g., $[\mathbf{8}]^*_2$) may be attributed to a combination of strong π-stacking interactions and intermolecular B···N dipole interactions that dominate in solution at high concentrations. However, upon dilution, these interactions become disfavored, and the excimer can dissociate to afford emission predominantly from the monomeric species. Interestingly, fluorescence emission from an excimer has never been observed for the monomeric BN-*n*-Bu-phenanthrene even at high concentrations,[16] which implies unique behavior for the dimeric system **8**. This excimer behavior is also in contrast to the all-

(31) (a) Förster, T. *Angew. Chem., Int. Ed. Engl.* **1969**, *8*, 333. (b) Berlman, I. B. *Handbook of Fluorescence Spectra of Aromatic Molecules*; Academic Press: New York, 1971.

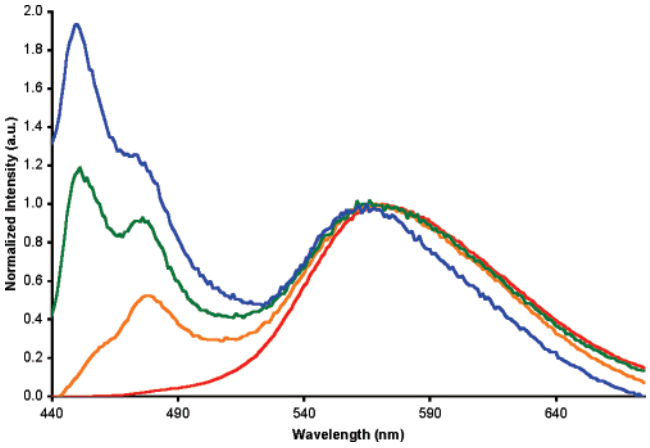

FIGURE 6. Fluorescence emission spectra of **8** at concentrations of 10^{-5} M (red), 10^{-6} M (orange), 10^{-7} M (green), and 10^{-8} M (blue). The spectral intensities are normalized to 1 at $\lambda = 566$ nm.

carbon phenanthrene, which fails to give excimer fluorescence[32] unless the chromophores are geometrically constrained in cyclophane-type arrangements.[33]

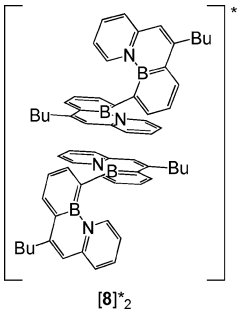

One other observation to note is that the low-energy excimer emission band in **8** was similar in location and appearance to the emission bands in **5**−**7**. This raised the possibility that the emission in **5**−**7** may actually result from excimer complexes as well. However, this possibility was excluded as emission bands from a monomeric species were never observed even at low concentrations where dimerization would be disfavored. In addition, excimers may be effectively prevented in **6** by the orthogonally positioned Ph groups, which may prevent close π-stacking interactions between phenanthrene moieties due to steric repulsion, whereas the *n*-Bu groups in **8** may be able to lie flat to allow such interactions to occur more readily.

(d) Fluorescence Emission of 9−**12.** Beginning with the case of the *n*-Bu derivatives, emission maxima were observed at 598 and 550 nm for species **9** and **10**, respectively (Figure 7), which are red-shifted by 55 and 7 nm relative to species **7** due to increased conjugation provided by an additional ethynyl group (**9**) or ethylene bridge (**10**). In addition, species **10** was red-shifted by 39 nm as compared to that of the monomeric BN-*n*-Bu-pyrene ($\lambda_{em} = 511$ nm, $\Phi_F = 0.16$),[15] which is suggestive of communication between the pyrene moieties. In the case of the Ph derivatives, emission maxima were observed at 630 and 521 nm for **11** and **12**, respectively. While the emission band for **11** was observed to be red-shifted by 62 nm as compared to

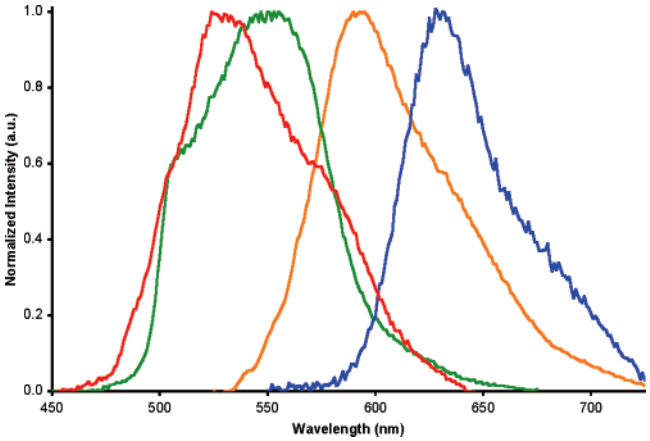

FIGURE 7. Fluorescence emission spectra of **9** (orange), **10** (green), **11** (blue), and **12** (red).

that of **5** due to increased conjugation from the additional ethynyl group, the emission band in **12** was found to be blue-shifted by 47 nm as compared to **5** and unchanged from that of the uncoupled BN-Ph-pyrene ($\lambda_{em} = 521$ nm, $\Phi_F = 0.11$).[15] These shifts suggest that **12** is less conjugated than **5** despite having a larger aromatic system and that there is no communication between the pyrene moieties in contrast to that observed in **10**. These observations may be explained by the molecular geometry, which may be directly influenced by the type of exocyclic substituent present. For example, it is likely that species **5** and **7**, as well as the ethynyl-substituted species **9** and **11**, would adopt a trans arrangement in which the exocyclic *n*-Bu and Ph substituents are pointing into opposite regions of space to minimize steric interactions. Thus, a coplanar arrangement between the phenanthrene moieties may result in enhanced communication between the chromophores and give rise to red-shifted emission bands from that of a single phenanthrene molecule due to extended conjugation. Conversely, the two pyrene moieties in species **10** and **12** would likely adopt a nearly orthogonal orientation to each other due to steric repulsion of the exocyclic substituents, which would result in reduced communication between the chromophores and a shorter effective conjugation length. Indeed, this was the case observed in the Ph derivative **12**, as the emission peaks were not red-shifted relative to the monomer, suggesting that the two pyrene moieties are orthogonal and act as independent chromophores. However, the *n*-Bu derivative **10** was observed to possess a red-shifted emission spectrum, which suggests that some degree of communication exists between the two chromophores. This may be explained by reduced steric interactions due to the smaller *n*-butyl groups that could reduce the amount of twist between the two chromophores and provide some extended conjugation. The quantum yield and lifetime were observed to be 0.06 and 20.5 ns for **10** and 0.12 and 25.8 ns for **12**, where the long lifetimes are consistent with those found in other BN-pyrene species.[15]

Conclusion

Through the simple substitution of ring C−C linkages by isoelectronic BN moieties, significant alteration of the photophysical properties was found to result for a series of species containing quaterphenyl molecular cores. While the photoluminescent efficiencies were observed to be well below that of *p*-quaterphenyl itself, the emission maxima were found to be

(32) Chandross, E. A.; Thomas, H. T. *J. Am. Chem. Soc.* **1972**, *94*, 2421.
(33) (a) Nakamura, Y.; Tsuihiji, T.; Mita, T.; Minowa, T.; Tobita, S.; Shizuka, H.; Nishimura, J. *J. Am. Chem. Soc.* **1996**, *118*, 1006. (b) Nakamura, Y.; Yamazaki, T.; Nishimura, J. *Org. Lett.* **2005**, *7*, 3259.

bathochromically shifted from the UV into the visible to afford fluorescence colors ranging from green to red. This strategy of BN heteroatom incorporation might provide an alternative method for tuning the emissive properties of quaterphenyl-based materials for use in optoelectronic devices. In addition, the observed electronic communication between the two phenanthrene or pyrene moieties suggests that conjugation could be further extended into the red or the near-IR (>700 nm) upon the successful synthesis of higher oligomers or polymeric species. In particular, near-IR fluorophores have attracted much attention for use as biologically relevant fluorescent probes, with a large emphasis placed upon the labeling and sensing of biomolecules, as well as in vivo diagnostic imaging.[34]

Experimental Section

All reactions and product manipulations were performed under an atmosphere of purified argon using vacuum line techniques or in a glovebox using dry solvents. See the Supporting Information for further details.

Synthesis of 1′ and 1. (a) A solution of 4,4′-bipyridine (0.012 g, 0.077 mmol) in toluene (3 mL) was added to a solution of **2,5-B** (0.036 g, 0.16 mmol) in toluene (3 mL) at 25 °C. The mixture was immediately diluted with hexanes (10 mL) and cooled to −35 °C, which afforded a minor amount of pale yellow crystals of **1′** over 2−3 weeks. Yield: 0.005 g (11%). (b) A solution of 4,4′-bipyridine (0.071 g, 0.045 mmol) in CH_2Cl_2 (5 mL) was added to a solution of **2,5-B** (0.205 g, 0.90 mmol) in CH_2Cl_2 (10 mL) at 25 °C. After 16 h, the volatiles were removed to afford **1** as a dark blue solid, which was washed with hexanes (2 × 10 mL) and dried in vacuo. X-ray quality crystals of **1** were obtained from slow evaporation of a CH_2Cl_2/hexanes (2:1) solution at 25 °C. Yield: 0.148 g (84%).

For **1′**: ^{1}H NMR (CD_2Cl_2): δ = 9.18 (d, J_{HH} = 7 Hz, H-3), 7.92 (d, J_{HH} = 7 Hz, H-2), 6.75 (br s, H-5), 6.15 (d, J_{HH} = 12 Hz, H-8), 5.82 (dd, J_{HH} = 12, 2 Hz, H-7), 2.82 (m, H-6), 1.99 (m, *i*Pr−CH), 0.97 (d, J_{HH} = 8 Hz, *i*Pr−Me), −0.12 (s, $SiMe_3$) ppm; ^{11}B{^{1}H} NMR (CD_2Cl_2): δ = 3.1 (br) ppm; ^{13}C{^{1}H} NMR (CD_2Cl_2, 233 K): δ = 150.4 (s, C-5), 146.1 (s, C-3), 144.2 (s, C-1), 136.7 (s, C-7), 133.7 (br s, C-8), 123.8 (s, C-2), 47.4 (s, C-6), 32.2 (s, *i*Pr−CH), 19.4 (s, *i*Pr−Me), −0.2 (s, $SiMe_3$) ppm, C-4 was not observed.

For **1**: ^{1}H NMR (CD_2Cl_2): δ = 9.07 (d, J_{HH} = 7 Hz, H-4), 7.82 (d, J_{HH} = 7 Hz, H-5), 7.35 (d, J_{HH} = 10 Hz, H-2), 6.73 (d, J_{HH} = 10 Hz, H-3), 2.85 (septet, J_{HH} = 7 Hz, *i*Pr−CH), 1.24 (d, J_{HH} = 7 Hz, *i*Pr−Me) ppm; ^{11}B{^{1}H} NMR (CD_2Cl_2): δ = 31.2 (br) ppm; ^{13}C{^{1}H} NMR (CD_2Cl_2): δ = 151.1 (s, C-6), 144.5 (s, C-4), 142.2 (s, C-1), 134.2 (s, C-5), 124.3 (s, C-2), 120.3 (br s, C-3), 35.4 (s, *i*Pr−CH), 25.5 (s, *i*Pr−Me); UV−vis (ϵ (10^4 L mol^{-1} cm^{-1})): λ_{max} (CH_2Cl_2) = 578 (0.6), 256 (1.4) nm; fluorescence (THF): no fluorescence was observed; ESI-MS (CH_2Cl_2, positive): m/z = 393 (M^+ + H, 10%).

Synthesis of 2′, 2, and 3. (a) Pyridine (0.155 g, 1.96 mmol) was condensed into a 60:40 mixture of **2,2′-B**/**4,4′-B** (0.125 g, 0.341 mmol) in CH_2Cl_2 (10 mL) at −78 °C. After 15 min, the mixture was warmed to 25 °C and stirred for 16 h. The volatiles were removed, and the resulting solid was washed with hexanes (30 mL) and dried in vacuo to afford a mixture of **2** and **3** as a dark purple solid. Yield: 0.079 g (75%). X-ray quality crystals of **3** (large red blocks) were obtained from CH_2Cl_2/hexanes (2:1) at −35 °C. Unfortunately, pure samples of **2** could not be obtained due to the presence of **3** as a consistent impurity. (b) When the previous reaction was performed in an NMR tube at 25 °C, the formation of **2′** and **3** was observed immediately. No attempt was made to try and isolate **2′**, which was characterized in situ by multi-nuclear NMR.

For **2′**: ^{1}H NMR (CD_2Cl_2, mixture of diastereomers ′ and ″): δ = 8.74 (dd, J_{HH} = 7, 1 Hz, H-3), 7.95 (br t, J_{HH} = 7 Hz, H-1), 7.55 (dd, J_{HH} = 8, 7 Hz, H-2), 6.99 (dd, J_{HH} = 3, 1 Hz, H-5′), 6.75 (dd, J_{HH} = 3, 2 Hz, H-5″), 6.64 (ddd, J_{HH} = 10, 2, 1 Hz, H-7′), 6.14 (dd, J_{HH} = 12, 2 Hz, H-8′), 5.62 (ddd, J_{HH} = 12, 3, 2 Hz, H-7″), 5.51 (dd, J_{HH} = 12, 2 Hz, H-8″), 3.33 (br s, H-6′), 3.29 (br s, H-6″), −0.20 (s, $SiMe_3$), −0.33 (s, $SiMe_3$) ppm; ^{11}B{^{1}H} NMR (CD_2Cl_2): δ = 3.0 (br s) ppm; ^{13}C{^{1}H} NMR (CD_2Cl_2, 253 K): δ = 155.9 (s, C-5′), 148.9 (s, C-5″), 146.8 (s, C-3), 143.1 (s, C-7′), 141.5 (s, C-1), 138.5 (br s, C-8′ + C-8″), 134.9 (s, C-7″), 127.3 (s, C-2), 47.3 (s, C-6′), 46.1 (s, C-6″), 0.03 (s, $SiMe_3$), 0.00 (s, $SiMe_3$) ppm, C-4 was not observed.

For **2**: ^{1}H NMR (CD_2Cl_2): δ = 9.07 (dd, J_{HH} = 7, 1 Hz, H-3), 8.01 (tt, J_{HH} = 6, 1 Hz, H-1), 7.70 (dd, J_{HH} = 7, 6 Hz, H-2), 7.60 (d, J_{HH} = 11 Hz, H-5), 6.70 (d, J_{HH} = 11 Hz, H-4) ppm; ^{11}B{^{1}H} NMR (CD_2Cl_2): δ = 31.3 (br) ppm; ^{13}C{^{1}H} NMR (CD_2Cl_2): δ = 144.4 (s, C-3), 140.2 (s, C-1), 135.3 (s, C-5), 126.9 (s, C-2), 119.5 (s, C-4) ppm, C-6 was not observed; UV−vis (ϵ (10^4 L mol^{-1} cm^{-1})): λ_{max} (CH_2Cl_2) = 385, 365, 330, 262 nm; fluorescence (THF): no fluorescence was observed.

For **3**: ^{1}H NMR (CD_2Cl_2): δ = 8.37 (dd, J_{HH} = 7, 2 Hz, H-3), 7.88 (tt, J_{HH} = 8, 2 Hz, H-1), 7.34 (t, J_{HH} = 7 Hz, H-2), 7.23 (dd, J_{HH} = 7, 1 Hz, H-7) 7.17 (ddd, J_{HH} = 10, 7, 1 Hz, H-5), 6.55 (td, J_{HH} = 7, 1 Hz, H-6), 6.15 (dd, J_{HH} = 10, 1 Hz, H-4) ppm; ^{11}B-{^{1}H} NMR (CD_2Cl_2): δ = 31.3 (br) ppm; ^{13}C{^{1}H} NMR (CD_2Cl_2): δ = 145.9 (s, C-3), 140.0 (s, C-1), 136.7 (s, C-7), 133.1 (s, C-5), 125.9 (s, C-2), 120.0 (br s, C-4), 117.7 (s, C-6) ppm, C-8 was not observed; UV−vis (ϵ (10^4 L mol^{-1} cm^{-1})): λ_{max} (THF) = 523 (0.1), 386 (0.2), 306 (0.4), 220 (0.8) nm; fluorescence (THF): no fluorescence was observed; ESI-MS (CH_2Cl_2, positive): m/z = 309 (M^+ + H, 100%).

Synthesis of 5 and 6. A solution of 2-(phenylethynyl)pyridine (0.034 g, 0.19 mmol) in CH_2Cl_2 (5 mL) was added to a 60:40 mixture of **2,2′-DBB** and **4,4′-DBB** (0.037 g, 0.10 mmol) in CH_2Cl_2 (10 mL) at 25 °C. After 3 days, the volatiles were removed, and the residue was dissolved in Et_2O/CH_2Cl_2 (10:1). The solution was loaded onto a short column of alumina, and elution with Et_2O then afforded a yellow band of **6**, which gave an orange solid after solvent removal. Yield: 0.020 g (65%). Subsequent elution with THF afforded an orange band of **5**, which gave a red solid after solvent removal: Yield: 0.014 g (67%). X-ray quality crystals of **6** were obtained by slow evaporation of Et_2O solution at 25 °C.

For **5**: ^{1}H NMR ($CDCl_3$): δ = 9.39 (d, J_{HH} = 7 Hz, H-12), 8.38 (dd, J_{HH} = 11, 1 Hz, H-5), 8.11 (d, J_{HH} = 1 Hz, H-2), 7.79 (d, J_{HH} = 12 Hz, H-4), 7.72 (d, J_{HH} = 9 Hz, H-9), 7.63 (dd, J_{HH} = 8, 2 Hz, H-14), 7.51−7.47 (m, H-10 + H-15 + H-16), 7.22 (s, H-7), 7.11 (td, J_{HH} = 7, 1 Hz, H-11) ppm; ^{11}B{^{1}H} NMR ($CDCl_3$): δ = 27.7 (br) ppm; ^{13}C{^{1}H} NMR ($CDCl_3$): δ = 155.5 (s, C-8), 142.8 (s, C-6), 142.1 (s, C-5), 141.3 (s, C-13), 137.5 (s, C-1), 135.8 (s, C-12), 130.1 (s, C-10), 130.0 (s, C-14), 129.2 (s, C-2), 128.3 (s, C-15), 127.7 (s, C-16), 127.2 (s, C-9), ca. 122 (br s, C-4), 115.5 (s, C-11), 114.0 (s, C-7) ppm, C-3 was not observed; UV−vis (ϵ (10^4 L mol^{-1} cm^{-1})): λ_{max} (cyclohexane) = 517 (4.8), 300 (6.6), 250 (6.2), 233 (6.5) nm; fluorescence (cyclohexane): λ_{max} = 568 nm, Φ_F = 0.16, τ_F = 4.0 ns; HR-MS for $C_{36}H_{26}N_2{}^{11}B_2$ (M^+): found 508.2282, calcd 508.2282.

For **6**: ^{1}H NMR ($CDCl_3$): δ = 9.64 (d, J_{HH} = 7 Hz, H-12), 7.85 (dd, J_{HH} = 8, 1 Hz, H-2/4), 7.74 (dd, J_{HH} = 7, 1 Hz, H-2/4), 7.71 (dd, J_{HH} = 7, 1 Hz, H-14), 7.68 (d, J_{HH} = 8 Hz, H-9), 7.58 (t, J_{HH} = 8 Hz, H-15), 7.52 (t, J_{HH} = 8 Hz, H-16), 7.32 (ddd, J_{HH} = 8, 7, 2 Hz, H-10), 7.16 (dd, J_{HH} = 8, 7 Hz, H-3), 6.48 (td, J_{HH} = 7, 2 Hz, H-11) ppm; ^{11}B{^{1}H} NMR ($CDCl_3$): δ = 29.1 (br) ppm; ^{13}C{^{1}H} NMR ($CDCl_3$): δ = 155.6 (s, C-8), 143.5 (s, C-6), 141.8 (s, C-13), 139.9 (s, C-2/4), 138.3 (s, C-12), 130.2 (s, C-10), 130.1 (s, C-14), 128.9 (s, C-2/4), 128.3 (s, C-15), 127.8 (s, C-16), 127.0 (s, C-9), 121.7 (s, C-3), 115.0 (s, C-11), 114.3 (s, C-7) ppm, C-1

(34) For reviews, see: (a) Fabian, J.; Nakazumi, H.; Matsuoka, M. *Chem. Rev.* **1992**, *92*, 1197. (b) Sevick-Muraca, E. M.; Houston, J. P.; Gurfinkel, M. *Curr. Opin. Chem. Biol.* **2002**, *6*, 642. (c) Tung, C. H. *Biopolymers* **2004**, *76*, 391. (d) Patonay, G.; Strekowski, L.; Raszkiewicz, A.; Kim, J. S. *Proc. SPIE—Int. Soc. Opt. Eng.* **2006**, *6097*, 609709.

and C-5 were not observed; UV−vis (ϵ (10^4 L mol^{-1} cm^{-1})): λ_{max} (cyclohexane) = 450 (1.2), 293 (2.2), 234 (1.9) nm; fluorescence (cyclohexane): λ_{max} = 591 nm, Φ_F = 0.02, τ_F = 4.5 ns; HR-MS for $C_{36}H_{26}N_2{}^{11}B_2$ (M^+): found 508.2324, calcd 508.2282.

Synthesis of 7 and 8. A solution of 2-(hex-1-ynyl)pyridine (0.047 g, 0.30 mmol) in CH_2Cl_2 (5 mL) was added to a 60:40 mixture of **2,2′-DBB** and **4,4′-DBB** (0.054 g, 0.15 mmol) in CH_2Cl_2 (10 mL) at 25 °C. After 16 h, the volatiles were removed, and the residue was dissolved/suspended in hexanes (5 mL). The suspension was filtered through a short column of alumina and washed with another 5 mL of hexanes. Elution with Et_2O afforded a yellow band of **8**, which gave an orange solid after solvent removal: Yield: 0.031 g (76%). Subsequent elution with THF afforded an orange band of **7**, which gave a red solid after solvent removal: Yield: 0.018 g (64%).

For **7**: ^{1}H NMR ($CDCl_3$): δ = 9.36 (d, J_{HH} = 7 Hz, H-12), 8.47 (dd, J_{HH} = 11, 1 Hz, H-5), 8.35 (d, J_{HH} = 1 Hz, H-2), 7.82 (d, J_{HH} = 12 Hz, H-4), 7.66 (d, J_{HH} = 9 Hz, H-9), 7.45 (td, J_{HH} = 8, 1 Hz, H-10), 7.13 (s, H-7), 7.05 (td, J_{HH} = 7, 1 Hz, H-11), 3.30 (m, H-13), 1.90 (pentet, J_{HH} = 7 Hz, H-14), 1.53 (sextet, J_{HH} = 7 Hz, H-15), 1.00 (t, J_{HH} = 7 Hz, H-16) ppm; ^{11}B{^{1}H} NMR ($CDCl_3$): δ = 27.6 (br) ppm; ^{13}C{^{1}H} NMR ($CDCl_3$): δ = 156.9 (s, C-8), 143.1 (s, C-6), 142.0 (s, C-5), 137.3 (s, C-1), 135.7 (s, C-12), 129.9 (s, C-10), 127.1 (s, C-2), 126.7 (s, C-9), ca. 123 (br s, C-4), 115.0 (s, C-11), 113.6 (s, C-7), 33.9 (s, C-13), 33.7 (s, C-14), 23.3 (s, C-15), 14.3 (s, C-16) ppm, C-3 was not observed; UV−vis (ϵ (10^4 L mol^{-1} cm^{-1})): λ_{max} (cyclohexane) = 512 (0.2), 490 (0.2), 290 (0.5), 230 (0.6) nm; fluorescence (cyclohexane): λ_{max} = 543, 558 nm, Φ_F = 0.05, τ_F = 3.5 ns; HR-MS for $C_{32}H_{34}N_2{}^{11}B_2$ (M^+): found 468.2900, calcd 468.2908.

For **8**: ^{1}H NMR ($CDCl_3$): δ = 9.48 (d, J_{HH} = 7 Hz, H-12), 8.08 (dd, J_{HH} = 8, 1 Hz, H-2/4), 7.69 (dd, J_{HH} = 7, 1 Hz, H-2/4), 7.58 (d, J_{HH} = 8 Hz, H-9), 7.22 (ddd, J_{HH} = 8, 7, 1 Hz, H-10), 7.19 (dd, J_{HH} = 8, 7 Hz, H-3), 7.13 (s, H-7), 6.33 (td, J_{HH} = 7, 2 Hz, H-11), 3.29 (m, H-13), 1.92 (pentet, J_{HH} = 7 Hz, H-14), 1.58 (sextet, J_{HH} = 7 Hz, H-15), 1.05 (t, J_{HH} = 7 Hz, H-16) ppm; ^{11}B-{^{1}H} NMR ($CDCl_3$): δ = 27.6 (br) ppm; ^{13}C{^{1}H} NMR ($CDCl_3$): δ = 156.6 (s, C-8), 143.7 (s, C-6), 139.4 (s, C-2/ 4), 138.2 (s, C-12), 129.8 (s, C-10), 126.3 (s, C-2/4), 121.1 (s, C-3), 114.3 (s, C-11), 113.8 (s, C-7), 34.0 (s, C-13), 33.8 (s, C-14), 23.4 (s, C-15), 14.3 (s, C-16) ppm, C-1 and C-5 were not observed; UV−vis (ϵ (10^4 L mol^{-1} cm^{-1})): λ_{max} (cyclohexane) = 446 (2.0), 288 (0.7), 235 (1.3) nm; fluorescence (cyclohexane): λ_{max} = 451, 475 (monomer), 566 (excimer) nm, Φ_F = 0.03 (monomer), 0.05 (excimer), τ_F = 4.3 (monomer), 23.3 (excimer) ns; HR-MS for $C_{32}H_{34}N_2{}^{11}B_2$ (M^+): found 468.2924, calcd 468.2908.

Acknowledgment. This work was funded by the Natural Science and Engineering Research Council (NSERC) of Canada in the form of a Discovery Grant to W.E.P. Alberta Ingenuity and NSERC are thanked for providing postdoctoral support to C.A.J. (2005−2007). The authors also thank Michael Bosdet for helpful discussions as well as Prof. Ray Turner (Calgary) for the use of his fluorimeter equipment.

Supporting Information Available: General experimental procedures and characterization data for **4**, **4′**, and **9**−**12**; molecular structure of **4′**; absorption and emission spectra for **5**−**12**; ^{1}H and ^{13}C{^{1}H} NMR spectra of **1′**, **1**, **3**, **4′**, and **5**−**12**; as well as crystallographic data for **1**, **3**, **4′**, and **6**. This material is available free of charge via the Internet at http://pubs.acs.org.

JO0706574